FERONIA functions through Target of Rapamycin (TOR) to negatively 1 2 regulate autophagy 3 Ping Wang¹, Natalie M. Clark², Trevor M. Nolan^{1,†}, Gaoyuan Song², Olivia G. Whitham¹, 4 Ching-Yi Liao¹, Christian Montes-Serey², Diane C. Bassham¹, Justin W. Walley^{2,3}, Yanhai 5 Yin^{1,3} and Hongging Guo^{1,*} 6 7 8 1 Department of Genetics, Development and Cell Biology, Iowa State University, Ames, Iowa 9 50011, USA 2 Department of Plant Pathology and Microbiology, Iowa State University, Ames, Iowa 50011, 10 11 **USA** 12 3 Plant Sciences Institutes, Iowa State University, Ames, Iowa 50011, USA 13 †Current Address: Department of Biology, Duke University, Durham, North Carolina 27708, 14 15 **USA** 16 *Author for correspondence: hguo@iastate.edu (H.G.) 17 Keywords: Autophagy, AZD8055, FERONIA, S6K1 phosphorylation, TOR 18 19 20 **Abstract** 21 FERONIA (FER) receptor kinase plays versatile roles in plant growth and development, biotic 22 and abiotic stress responses, and reproduction. Autophagy is a conserved cellular recycling 23 process that is critical for balancing plant growth and stress responses. Target of Rapamycin 24 (TOR) has been shown to be a master regulator of autophagy. Our previous multi-omics analysis 25 with loss-of-function fer-4 mutant implicated that FER functions in the autophagy pathway. We 26 further demonstrated here that the fer-4 mutant displayed constitutive autophagy, and FER is required for TOR kinase activity measured by S6K1 phosphorylation and by root growth 27 28 inhibition assay to TOR kinase inhibitor AZD8055. Taken together, our study provides a previously unknown mechanism by which FER functions through TOR to negatively regulate 29 30 autophagy.

INTRODUCTION

32

33

34 like (CrRLK1L) subfamily. FER functions together with co-receptors LLGs/LRE, cell wall 35 components, such as LRX proteins and pectin, and ligands such as RALFs to regulate many 36 downstream signaling components to play essential roles in plant growth and development, 37 reproduction and stress responses (Boisson-Dernier et al., 2011; Lindner et al., 2012; Haruta et 38 al., 2014; Li et al., 2016; Franck et al., 2018; Zhao et al., 2018; Duan et al., 2020; Solis-Miranda 39 and Quinto, 2021; Lin et al., 2022; Xie et al., 2022). FER was first identified for its crucial role 40 in female reproduction, as loss-of-function fer mutants displays reduced fertility due to pollen 41 tube overgrowth (Escobar-Restrepo et al., 2007). FER was also required for optimal vegetative growth (Guo et al., 2009) and root hair development (Duan et al., 2010). Subsequent studies 42 43 revealed more functions of FER, including plant hormone Abscisic Acid (ABA) signaling (Yu et 44 al., 2012), cold and heat stress responses (Chen et al., 2016), salt stress response (Feng et al., 45 2018; Zhao et al., 2018; Gigli-Bisceglia and Testerink, 2021), photooxidative stress (Shin et al., 46 2021), mechano-sensing (Shih et al., 2014; Tang et al., 2022), thigmomorphogenesis (Darwish et 47 al., 2022) and immune responses to bacterial pathogens (Keinath et al., 2010; Stegmann et al., 48 2017; Guo et al., 2018), fungal pathogens (Kessler et al., 2010; Masachis et al., 2016) and 49 nematodes (Zhang et al., 2020). Recent study showed that FER-mediated ROS production 50 regulates levels of beneficial pseudomonads in the rhizosphere microbiome, independent of 51 FER's immune function (Song et al., 2021). Our most recent study also revealed novel functions 52 of FER in the negative regulation of Endoplasmic Reticulum (ER) body formation and 53 glucosinolate biosynthesis (Wang et al., 2022). 54 Autophagy, meaning "self-eating", is a conserved cellular recycling process that employs 55 specialized vesicles to encapsulate and deliver cytoplasmic material to the vacuole for 56 degradation. Cargoes including single macromolecules, large macromolecular complexes such as ribosomes and proteasomes, protein aggregates, damaged or whole organelles, and even invading 57 58 pathogens can be eliminated through autophagy in bulk or selectively (Liu and Bassham, 2012; 59 Marshall and Vierstra, 2018). This autophagic process is critical for removing non-functional 60 molecules within the cell and replenishing the nutrient sources for new growth, and it is also important for regulating specific biological processes or signaling pathways by selectively 61 62 degrading specific cargoes (Zhou et al., 2014; Nolan et al., 2017; Zhuang et al., 2018; Xia et al.,

FERONIA (FER) is a receptor-like kinase (RLK) and belongs to the Catharantus roseus RLK1-

2020; Lin et al., 2021; Luo et al., 2021; Wang et al., 2021; Liao et al., 2022). Thus, autophagy plays important roles in plant growth and development and stress responses to facilitate plant tolerance and survival under unfavorable conditions (Marshall and Vierstra, 2018). In plants, autophagy is maintained at a basal level during growth and development to ensure homeostasis, but it is upregulated under environmental stresses to aid plant survival (Wang et al., 2018). The autophagy process starts with induction by upstream kinases, following by cargo recognition, phagophore formation, phagophore expansion and closure, autophagosome fusion and breakdown in vacuoles (Marshall and Vierstra, 2018).

The core machinery of autophagy is conserved among eukaryotes and is mainly regulated by two energy sensors, Sucrose Non-Fermenting (SNF)-related kinase 1 (SnRK1) and Target of Rapamycin (TOR). In Arabidopsis, SnRK1 is required for autophagy induction under a wide variety of stress conditions (Soto-Burgos and Bassham, 2017). SnRK1 activates autophagy through direct phosphorylation of ATG1 and through inhibition of TOR activity, and functions upstream of TOR (Chen et al., 2017; Soto-Burgos and Bassham, 2017). In contrast, TOR kinase functions as a negative regulator of plant autophagy (Liu and Bassham, 2010). In the case of TOR inactivation, the transcripts of many autophagy-related genes (*ATGs*) were significantly upregulated in Arabidopsis, leading to the activation of autophagy machinery (Liu et al., 2012; Dong et al., 2015). In yeast and Arabidopsis, TOR regulates autophagy through direct phosphorylation of ATG13 (Alers et al., 2012; Son et al., 2018; van Leene et al., 2019).

FER and TOR have both been shown to positively regulate plant growth. Very recently, the crosstalk between FER-mediated signaling and TOR-mediated nutrient/energy metabolism has been reported, which revealed that FER interacts with the TOR pathway to regulate nitrogen-related nutrient signaling under low nutrient conditions (Song et al., 2022). However, how FER regulates autophagy and whether or not this regulation is through TOR is unknown. In this study, we investigated autophagy phenotype of *fer-4* mutant, and our genetic studies showed strong interaction between FER and TOR in plant growth and autophagy. We further found that FER is required for TOR kinase activity. Our results showed that FER functions through TOR to negatively regulate autophagy.

94 **Plant Materials and Growth Conditions** 95 The Arabidopsis accession Columbia-0 was used as WT in all experiments. T-DNA insertion mutants fer-4 (GABI-106A06), TOROE (GABI 548G07), raptor1b (SALK 078159), s6k1 96 97 (SALK 148694) were described previously (Anderson et al., 2005; Deprost et al., 2007; 98 Henriques et al., 2010; Ren et al., 2011; Guo et al., 2018). GFP-ATG8e overexpression line was 99 previously described (Xiong et al., 2007). For all experiments involving Arabidopsis plants, seeds were sterilized with 70% ethanol containing 0.1% Triton and germinated on ½ Linsmainer 100 101 & Skoog (LS) plates with 1% sucrose and 0.7% agar, with or without treatments as indicated 102 when it is appropriate. 10-day old seedlings were transferred into soil at 22°C under long-day (16 103 h light/8 h dark) conditions with a photon fluence rate of \sim 120 µmol m⁻²s⁻¹. 104 105 Sucrose starvation and autophagosome observation 106 For autophagosome observation and quantification, 7-day-old seedlings grown under constant 107 light were transferred to control ½ LS plates with 1% sucrose and starvation plates without 108 sucrose, and incubate in dark for three days. GFP-ATG8e-labeled autophagosomes were 109 observed and counted by epifluorescence microscopy using a fluorescein isothiocyanate (FITC) 110 filter. Representative GFP-labeled autophagosome images were taken by confocal microscopy 111 using a Zeiss Laser Scanning Microscope 700 (LSM700) with a 63×oil immersion objective. 112 GFP was excited with a 488 nm laser line and detected from 555 nm. 113 114 **AZD8055** treatment 115 For root growth inhibition assay, sterilized seeds were germinated on control ½ LS or plates 116 containing 1 µM AZD8055 for 7 days under constant light. The plates were scanned and the root 117 lengths were measured using ImageJ. 118 For short term AZD8055 treatment for western blotting, 10-day-old seedlings grown on 119 ½ LS plates were transferred to control liquid ½ LS or ½ LS with AZD8055 for the amount of 120 time indicated in each experiment. The seedlings were collected and dabbed dry and flash frozen 121 in liquid nitrogen. The samples were ground in 2xSDS buffer (100 mM Tris-HCl pH 6.8, 4% 122 (w/v) SDS, 20% (v/v) glycerol, 0.2% (w/v) bromophenol blue, 0.2 M β-mercaptoethanol) and

93

MATERIALS AND METHODS

123 used for immunoblot analysis using anti-S6K1/2 antibody (Agrisera, AS121855). The relative 124 intensity of P-S6K and S6K were quantified using ImageJ. 125 For short term AZD8055 treatment for autophagosome observation, 7-day-old seedlings 126 of WT GFP-ATG8e and fer-4 GFP-ATG8e grown on ½ LS plates were transferred to control 127 liquid ½ LS or ½ LS with 1 µM AZD8055 for 6 hours before observation under an 128 epifluorescence microscope. 129 130 **GFP-ATG8e** cleavage assay 131 Seven-day-old WT GFP-ATG8e and fer-4 GFP-ATG8e seedlings were subjected to ½ LS liquid 132 medium without sucrose for 6, 12, and 24 hours in dark, or to ½ LS liquid with or without 1 μM 133 AZD8055 for 6 hours in light before harvesting. Total protein was isolated with 2xSDS buffer 134 (100 mM Tris-HCl pH 6.8, 4% (w/v) SDS, 20% (v/v) glycerol, 0.2% (w/v) bromophenol blue, 135 0.2 M β-mercaptoethanol) and resolved on 10% SDS-PAGE gels for immunoblot analysis using 136 monoclonal anti-GFP antibody (Sigma-Aldrich, MAB3836). The relative intensity of GFP-137 ATG8e and free GFP were quantified using ImageJ. 138 139 Protoplast isolation and transient expression assays 140 Leaves of 4-week-old Col-0 and raptor 1b plants grown under long-day conditions were collected and peeled for protoplast isolation as previously described (Wu et al., 2009; Yoo et al., 2007). 141 142 Protoplasts were resuspended in MMg solution (400 mM mannitol, 15 mM MgCl₂, and 4 mM 143 MES pH5.7). Plasmids of 35S:GFP control, 35S:FER-GFP and 35S:mCherry-ATG8e were 144 prepared using Maxiprep kits (Sigma-Aldrich, NA0310) and set the final concentration at 1 145 μg/μL. Ten micrograms of each plasmid was introduced into 200 μL protoplasts by adding 220 146 μL of PEG solution (40% PEG4000, 200 mM mannitol, and 100 mM CaCl₂). After 147 transformation, protoplasts were washed and incubated in 1 mL of W5 solution (154 mM NaCl, 148 125 mM CaCl₂, 5 mM KCl, 2 mM MES pH5.7) overnight. 149 For sucrose starvation, protoplasts were incubated in W5 solution without sucrose or with 150 0.5% (w/v) sucrose as control for 36 hours at room temperature. For constitutive autophagy in 151 raptor 1b mutant, protoplasts were incubated in W5 solution only for 20 hours. Protoplasts were 152 observed using an epifluorescence microscope (Carl Zeiss Axio Imager.A2, Germany) with 153 TRITC filter. Protoplasts with more than three visible autophagosomes were counted as being

154 active for autophagy. A total of 100 well-expressed protoplasts were observed per treatment per 155 genotype, and the percentage of protoplasts with active autophagy was quantified and averaged 156 from 3-4 independent replicates (Wang et al., 2021). 157 158 Generalized linear model 159 To specifically examine the genotype-by-treatment interaction to determine the sensitivity of the 160 fer-4, TOROE, and fer-4 TOROE to AZD treatment, we used a generalized linear model (glm package in R) with genotype and treatment (Control or AZD) as fixed factors. Genotypes were 161 162 categorized as significantly differentially responsive to AZD if they had a genotype-by-treatment 163 interaction p-value < 0.05 compared to all other lines. 164 165 Statistical analysis 166 Graphs were created in GraphPad Prism software (version 9.3.0). SPSS version 27.0 software 167 (IBM, Armonk, NY, USA) was used for statistical data analysis. The data are shown as 168 means \pm standard error of the mean (SEM) and were subjected to one-way analysis of variance 169 (ANOVA) Tukey's multiple range tests (p < 0.05). 170 171 **RESULTS** 172 173 FER negatively regulates autophagy 174 Our recently published multi-omics analysis of the loss-of-function fer-4 mutant revealed that the 175 Gene Ontology term, autophagy (GO:0006914) is enriched (Wang et al., 2022), suggesting that 176 FER plays a role in autophagy regulation. We then compared fer-4 transcriptome and proteome 177 to autophagy-related genes (Homma et al., 2011). The analysis revealed that about 36% (77/212) 178 of the genes known to be involved in plant autophagy have altered levels of transcripts or 179 proteins in fer-4 mutant (Figure 1A; Supplemental Table 1). Closer examination showed that at 180 least 16 genes with known functions in autophagy have altered transcripts or protein levels in 181 fer-4, including many autophagy-related genes (ATGs), Target of Rapamycin (TOR) and 182 Regulatory-associated protein of TOR 1B (RAPTOR1B) (Figure 1B). 183 To gain a better understanding of the role FER plays in autophagy, we crossed GFP-ATG8e transgenic plants with fer-4 mutant to generate fer-4 GFP-ATG8e. ATG8e is localized on 184

the autophagic membranes and can serve as a reliable marker for autophagosome observation and quantification (Contento et al., 2005). We carried out sucrose starvation followed by autophagosome quantification in 10-day-old Arabidopsis seedlings.

While very few autophagosomes were evident in *WT GFP-ATG8e* under normal growth conditions, the number was substantially increased by sucrose starvation. Interestingly, the *fer-4 GFP-ATG8e* displayed constitutive autophagy, with significantly increased levels of autophagosomes under both normal and starvation conditions (Figure 2A, 2B). The results indicated that FER functions to suppress autophagy pathway. To further support that FER functions to inhibit autophagy pathway, we generated a second FER mutant allele, *FER-miRNA/GFP-ATG8e*, by overexpressing *FER-miRNA* in *WT GFP-ATG8e* plants. *FER-miRNA* is highly effective in knocking down the endogenous FER (Guo et al., 2009; Wang et al., 2022). Three T2 transgenic lines (*FER-miRNA/GFP-ATG8e #1, #2, #4*), in which the FER protein levels were significantly decreased, were used for sucrose starvation followed by autophagosome quantification (Figure 2C). Similar to *fer-4 GFP-ATG8e*, all three lines had higher levels of autophagosomes than *WT GFP-ATG8e* under both nutrient-rich (SUC+) and sucrose starvation (SUC-) conditions (Figure 2D).

Upon autophagosome fusion with vacuole, the GFP-ATG8e protein is delivered to vacuole where it is degraded to release a free and relatively stable GFP; and the free GFP/GFP-ATG8e ratio reflects the level of autophagy activity (Chen et al., 2017; Li et al., 2014). Sevenday-old *WT GFP-ATG8e* and *fer-4 GFP-ATG8e* seedlings were treated in sucrose-free ½ LS medium in dark for 0, 6, 12 and 24 hours. As shown in Figure 2E, the release of free GFP was readily observed in both WT and *fer-4* mutant plants upon carbon starvation, whereas the free GFP/GFP-ATG8e ratios in the *fer-4* mutant were higher than that in WT, even at 0 hour control condition, suggesting that there was constitutive autophagy in *fer-4* mutant and depletion of FER enhances autophagic activity. These results demonstrated that FER negatively regulates autophagy.

TOR is a negative regulator of autophagy in plants (Liu and Bassham, 2010) and its kinase inhibitor AZD8055 was used to induce autophagy by suppressing TOR activity (Dong et al., 2015; Pu et al., 2017). We also applied 1 µM AZD8055 to 7-day-old *WT GFP-ATG8e* and *fer-4 GFP-ATG8e* seedlings for 6 hours for autophagosomes observation and GFP-ATG8e cleavage assay. Similar to sucrose starvation, the *fer-4 GFP-ATG8e* had significantly more

216 autophagosomes (Figure 3A) and higher free GFP/GFP-ATG8e ratios (Figure 3B) than WT 217 GFP-ATG8e under both control and AZD8055 treatment conditions. These results further 218 supports that FER negatively regulates autophagy. 219 220 FER is required for TOR kinase activity 221 TOR is an atypical Ser/Thr kinase of the phosphatidylinositol 3-kinase-related lipid 222 kinase family. Similar to its counterparts in yeast and mammals, TOR functions in a complex 223 with RAPTOR and LST8 and plays central roles in balancing nutrient, energy, and internal and 224 external stimuli to regulate plant growth development and stress responses (Shi et al., 2018). The 225 fact that both TOR and FER positively regulate plant growth and negatively regulate autophagy 226 (Figures 2-3; Deprost et al., 2007; Guo et al., 2009; Liu and Bassham, 2010; Pu et al., 2017; 227 Soto-Burgos and Bassham, 2017) prompted us to examine their interactions more closely. 228 The comparison of genes mis-expressed in fer-4 (Wang et al., 2022) and the genes 229 regulated by AZD8055 (Dong et al., 2015) revealed that a large number of TOR-dependent 230 genes (40% of AZD-repressed, p < 0.001; 42% of AZD-induced, p < 0.001) are regulated by 231 FER (Figure 4A, 4B). Interestingly, majority of the 40% of AZD-repressed genes (86%, p <0.001) have decreased transcript levels in fer-4, and majority of the 42% of AZD-induced genes 232 233 (93%, p < 0.001) have increased transcript levels in fer-4, which suggests a corporative 234 relationship between FER and TOR (Figure 4A, 4B; Supplemental Tables 2-3). Comparisons 235 with differentially expressed proteins in fer-4 gave similar results (Figure 4A; Supplemental 236 Tables 2-3). We also compared AZD8055 regulated genes with two other sets of published 237 transcriptome data of fer-4, one was from 10-day-old seedlings in Wang et al. (2022) and another 238 was in Guo et al. (2018). The amount of overlaps are very similar, which further strengthened 239 our observation that FER and TOR interact in a cooperative manner (Supplemental Figure 1). 240 We further constructed the double mutant fer-4 TOROE GFP-ATG8e, where TOROE is a 241 TOR overexpression T-DNA insertional mutant (Deprost et al., 2007). While the TOROE mutant 242 growth phenotype is similar to that of WT and has decreased autophagy induction by sucrose 243 starvation, fer-4 TOROE GFP-ATG8e mirrors fer-4 GFP-ATG8e, with stunted growth and 244 constitutive autophagy (Figure 4C-4E), which suggests that either FER is epistatic to TOR or 245 TOR activity requires FER.

246 To clarify the genetic relationship between FER and TOR, we carried out a transient 247 assay by co-expressing FER-GFP and autophagy marker mCherry-ATG8e in protoplasts. We 248 first found that FER-GFP transient expression in Col-0 protoplasts could dramatically inhibit 249 autophagy induction by sucrose starvation (Figure 5A). There was constitutive autophagy in 250 raptor1b protoplasts even without any treatment compared with WT (Figure 5B; Pu et al., 2017). 251 However, FER-GFP overexpression could not inhibit such constitutive autophagy in raptor1b 252 (Figure 5B), suggesting that RAPTOR1B functions downstream of FER. This result suggests that 253 TOR/RAPTOR1B complex functions downstream of FER, and the previous observation in the 254 fer TOROE double mutant is likely due to that FER is required for TOR activity. 255 To further clarify that TOR requires FER for its activity, we carried out a root growth 256 inhibition assay in response to TOR kinase inhibitor AZD8055. After growing on control ½ LS 257 plates or plates containing 1 µM AZD8055 for 7 days, WT root growth was inhibited by 1 µM 258 AZD8055 to 36% of the control treatment, while fer-4 was hypersensitive to the inhibitor 259 treatment, with root growth decreased to 27% of the control, suggesting decreased TOR activity 260 in fer-4 mutant. As expected, TOROE is less sensitive to AZD8055 than that of WT with 41% 261 growth, and fer-4 TOROE double mutant is more sensitive to the inhibitor, with 26% growth of 262 the control, similar to fer-4 mutant (Figure 6A, 6B). 263 To ascertain that fer-4 TOROE responded in a similar fashion to fer-4 single mutant in 264 AZD8055-mediated root inhibition, we also analyzed the responses of WT, fer-4, TOROE, and 265 fer-4 TOROE to AZD8055 using a generalized linear model (glm package in R) with genotype 266 and treatment (Control or AZD) as fixed factors. Similar results were obtained that fer-4 and fer-267 4 TOROE are more sensitive to AZD8055 treatment while TOROE is more resistant to the 268 treatment significantly (Figure 6C). 269 S6K1/2, P70 ribosomal S6 kinases, are substrates of TOR kinase and their 270 phosphorylation status can be used as an indicator of TOR kinase activity (Mahfouz et al., 2006). 271 To further examine TOR activity in the fer-4 mutant, we obtained anti-S6K1/2 and anti-P-272 S6K1/2 antibodies from Agrisera and tested in WT with and without AZD8055 treatment. While 273 anti-P-S6K1/2 antibody only recognized the phosphorylated S6K1/2, anti-S6K1/2 antibody 274 recognized both phosphorylated and non-phosphorylated S6K1/2 (Figure 7A). AZD8055 (5 μM) 275 treatment for three hours completely diminished the phosphorylated S6K1/2 (Figure 7A), 276 confirming that S6K phosphorylation can be used as a readout of TOR activity. The anti-S6K1/2

antibody can recognize both forms of S6K1 and has high specificity since very little signal (likely from S6K2) was observed in *s6k1* mutant (Figure 7B), and it was therefore used for subsequent experiments.

Western blotting was carried out using 10-day-old seedlings with and without treatment of different AZD8055 concentrations for one hour. Compared to WT, *fer-4* mutant has decreased TOR kinase activity, with lowered P-S6K1/S6K1 ratio. The *raptor1b* mutant, where TOR activity is severely compromised, has no detectable phosphorylated S6K1 (Figure 7B). The TOR OE plants have relatively higher P-S6K1/S6K1 ratio than that in WT after AZD8055 treatment (Supplemental Figure 2). We further examined the TOR kinase activity in *fer-4 TOROE* double mutant. Under normal growth conditions supplemented with sucrose, while *fer-4* has decreased and *TOROE* has elevated TOR kinase activity, the double mutant behaves like *fer-4*, with decreased TOR kinase activity reflected by lowered P-S6K1/S6K1 ratio, compared to WT control. Sucrose starvation for three days decreased both forms of the S6K1 protein level (Figure 7C). Taken together, these results support the hypothesis that FER is required for TOR kinase activity and its normal function.

In summary, our results demonstrated that FER is required for TOR kinase activity, and FER functions through TOR kinase to negatively regulate autophagy (Figure 7D). Thus, our results provide novel insights into the regulation of autophagy by a plasma membrane-localized receptor-like kinase FER.

DISCUSSION

FER receptor kinase is a versatile regulator and mediates many important biological processes in plant growth, development and stress responses. Our recent integrated omics analysis of *fer-4* mutant not only confirmed the previous known FER functions but also revealed novel pathways regulated by FER and underlying molecular mechanisms, such as ER body formation, indole glucosinolate biosynthesis and ABA responses (Wang et al., 2022). In this study, we further expanded the findings and provided genetic, molecular and cell biological evidence that FER is involved in autophagy regulation. Consistent with the significant overlaps between autophagy genes and those affected in *fer-4* mutant (Figure 1), *fer* mutants displayed constitutive autophagy phenotype under normal condition, sucrose starvation and AZD8055 treatments (Figures 2-3). Further genetic, cell biology and biochemical assays showed that FER is required for TOR

kinase activity (Figures 4-7). Our results indicated that FER functions through TOR to negatively regulate autophagy.

As a conserved cellular process, autophagy plays important roles in recycling cytosolic material and maintaining cellular homeostasis during growth, development and responses to diverse environmental stresses. TOR, as an essential serine/threonine kinase, is a master regulator of autophagy. From cargo selection to the destination vacuole, autophagy involves many steps, and TOR plays important roles in integrating the nutrient and energy signals to initiate autophagy (Liu and Bassham, 2012; Marshall and Vierstra, 2018; Soto-Burgos et al., 2018). Despite all of the progress, how TOR is regulated by signaling pathways is less known. This study provides new insights into how TOR is regulated by a plasma membrane-localized receptor kinase, capable of integrating internal and external stimuli, to regulate autophagy.

FER has been shown to physically interact with TOR kinase complex (Martínez Pacheco et al., 2022; Song et al., 2022). It is conceivable that FER and TOR also directly interact during autophagy regulation. Another possible mechanism by which FER regulates TOR kinase activity is through a Rho GTPase, ROP2. ROP2 has been shown to directly interact and activate TOR in response to auxin and light (Li et al., 2017; Schepetilnikov et al., 2017). FER was shown to directly interact with ROP2 and activate ROP2-mediated signaling (Duan et al., 2010). It is also conceivable that FER functions in the same complex with ROP2 and TOR, and thus activates TOR kinase.

We previously observed that TOR and RAPTOR1B protein levels were increased in *fer-4* mutant (Figure 1B) while TOR has reduced activity in the mutant (Figures 6-7). This seemingly conflicting observation could be due to the possibility that kinase activity is negatively correlated to its protein stability, lower TOR kinase activity stabilizes the protein. This is also observed in the case of FERONIA kinase. When transiently expressed in *Nicotiana Benthamiana*, FER^{K565R}, an inactive kinase accumulated to much higher levels compared to the wild-type FER (Guo et al., 2018; Wang et al., 2022). When transformed to *fer-4* for complementation, FER^{K565R} protein levels are in general higher that wild-type FER, whereas FER^{K565R} could not complement the mutant to the same extent as the wild-type FER (Chakravorty et al., 2018).

Our multi-omics data analysis with *fer-4* mutant produced many enriched GO terms related to nutrient and energy production and metabolism (Wang et al., 2022), suggesting that FER plays important roles in nutrient and energy homeostasis. Our study therefore suggests an

339	exciting possibility that FER and TOR function together to gauge nutrient and energy levels and
340	regulate autophagy induction. Consistent with this possibility, a recent study showed that
341	RALF1-FER complex interacts with and activates TOR signaling in response to nitrogen
342	starvation (Song et al., 2022). FER regulates diverse biological processes, and autophagy is a
343	critical cellular recycling process involved in plant growth development and stress responses. We
344	show here that FER is required for TOR kinase activity and FER functions through TOR to
345	regulate autophagy. How FER/TOR-regulated autophagy is involved in FER-regulated biological
346	processes will be interesting for future studies.
347	
348	AUTHOR CONTRIBUTIONS
349	H.G. conceived the project. H.G. and P.W. performed genetic, molecular, biochemical, and cell
350	biology analysis. G.S. performed proteomics. N.M.C., G.S., and T.M.N. performed the omics
351	data analysis. N.M.C. performed statistical analysis for transcript and protein enrichment. D.C.B.
352	and C.L. contributed to data analysis. H.G. and P.W. wrote the manuscript, with edits or input
353	from other co-authors.
354	
355	FUNDING
356	This work was supported by grants from National Institute of Health (NIH 1R01GM120316-
357	01A1 to Y.Y., D.C.B., and J.W.W.), National Science Foundation (NSF MCB-1818160 to Y.Y.
358	and J.W.W.), and Plant Sciences Institute at Iowa State University (to Y.Y. and J.W.W.).
359	
360	CONFLICT OF INTEREST
361	H.G. and Y.Y. are co-inventors on the patent US9512440B2, titled "Modulation of receptor-like
362	kinase for promotion of plant growth."
363	Conflict of interest statement. None declared.
364	
365	REFERENCES
366	Alers, S., Löffler, A. S., Wesselborg, S., and Stork, B. (2012). Role of AMPK-mTOR-Ulk1/2 in
367	the Regulation of Autophagy: Cross Talk, Shortcuts, and Feedbacks. Mol. Cell. Biol. 32, 2-
260	11. doi: 10.1128/mch.06150.11

- Anderson, G. H., Veit, B., and Hanson, M. R. (2005). The Arabidopsis AtRaptor genes are
- essential for post-embryonic plant growth. *BMC Biol.* 3. doi: 10.1186/1741-7007-3-12.
- Boisson-Dernier, A., Kessler, S. A., and Grossniklaus, U. (2011). The walls have ears: The role
- of plant CrRLK1Ls in sensing and transducing extracellular signals. J. Exp. Bot. 62, 1581–
- 373 1591. doi: 10.1093/jxb/erq445.
- Chakravorty, D., Yu, Y., and Assmann, S. M. (2018). A kinase-dead version of FERONIA
- receptor-like kinase has dose-dependent impacts on rosette morphology and RALF1-
- mediated stomatal movements. *FEBS Lett.* 592, 3429-3437. doi: 10.1002/1873-3468.13249.
- 377 Chen, J., Yu, F., Liu, Y., Du, C., Li, X., Zhu, S., et al. (2016). FERONIA interacts with ABI2-
- 378 type phosphatases to facilitate signaling cross-talk between abscisic acid and RALF peptide
- in Arabidopsis. *Proc. Natl. Acad. Sci. USA* 113, E5519–E5527. doi:
- 380 10.1073/pnas.1608449113.
- 381 Chen, L., Su, Z. Z., Huang, L., Xia, F. N., Qi, H., Xie, L. J., et al. (2017). The AMP-activated
- protein kinase kin10 is involved in the regulation of autophagy in arabidopsis. *Front. Plant*
- 383 *Sci.* 8. doi: 10.3389/fpls.2017.01201.
- Contento, A. L., Xiong, Y., and Bassham, D. C. (2005). Visualization of autophagy in
- Arabidopsis using the fluorescent dye monodansylcadaverine and a GFP-AtATG8e fusion
- protein. *Plant J.* 42, 598–608. doi: 10.1111/j.1365-313X.2005.02396.x.
- Darwish, E., Ghosh, R., Ontiveros-Cisneros, A., Cuong Tran, H., Petersson, M., de Milde, L., et
- al. (2022). Touch signaling and thigmomorphogenesis are regulated by complementary
- CAMTA3-and JA-dependent pathways. *Sci. Adv.* 8, eabm2091. doi:
- 390 10.1126/sciadv.abm2091.
- Deprost, D., Yao, L., Sormani, R., Moreau, M., Leterreux, G., Bedu, M., et al. (2007). The
- Arabidopsis TOR kinase links plant growth, yield, stress resistance and mRNA translation.
- 393 *EMBO Rep.* 8, 864–870. doi: 10.1038/sj.embor.7401043.
- Dong, P., Xiong, F., Que, Y., Wang, K., Yu, L., Li, Z., et al. (2015). Expression profiling and
- functional analysis reveals that TOR is a key player in regulating photosynthesis and
- 396 phytohormone signaling pathways in Arabidopsis. Front. Plant Sci. 6. doi:
- 397 10.3389/fpls.2015.00677.

- Duan, Q., Kita, D., Li, C., Cheung, A. Y., and Wu, H. M. (2010). FERONIA receptor-like kinase
- regulates RHO GTPase signaling of root hair development. *Proc. Natl. Acad. Sci. USA* 107,
- 400 17821–17826. doi: 10.1073/pnas.1005366107.
- 401 Duan, Q., Liu, M. C. J., Kita, D., Jordan, S. S., Yeh, F. L. J., Yvon, R., et al. (2020). FERONIA
- 402 controls pectin- and nitric oxide-mediated male–female interaction. *Nature* 579, 561–566.
- 403 doi: 10.1038/s41586-020-2106-2.
- 404 Escobar-Restrepo, J.M., Huck, N., Kessler, S., Gagliardini, V., Gheyselinck, J., Yang, W.C., et
- al. (2007). The FERONIA receptor-like kinase mediates male-female interactions during
- pollen tube reception. *Science* (1979) 317, 656--660. doi: 10.1126/science.1143964.
- 407 Feng, W., Kita, D., Peaucelle, A., Cartwright, H. N., Doan, V., Duan, Q., et al. (2018). The
- FERONIA Receptor Kinase Maintains Cell-Wall Integrity during Salt Stress through Ca2+
- 409 Signaling. Curr. Biol. 28, 666-675.e5. doi: 10.1016/j.cub.2018.01.023.
- 410 Franck, C. M., Westermann, J., and Boisson-Dernier, A. (2018). Plant Malectin-Like Receptor
- Kinases: From Cell Wall Integrity to Immunity and Beyond RLK: receptor-like kinase.
- 412 Annu. Rev. Plant Biol. 69, 301-328. doi: 10.1146/annurev-arplant-042817.
- 413 Gigli-Bisceglia, N., and Testerink, C. (2021). Fighting salt or enemies: shared perception and
- signaling strategies. Curr. Opin. Plant Biol. 64, 102120. doi: 10.1016/j.pbi.2021.102120.
- Guo, H., Li, L., Ye, H., Yu, X., Algreen, A., and Yin, Y. (2009). Three related receptor-like
- kinases are required for optimal cell elongation in Arabidopsis thaliana. *Proc. Natl. Acad.*
- 417 *Sci. USA* 106, 7648-7653. doi: 10.1073/pnas.0812346106.
- 418 Guo, H., Nolan, T. M., Song, G., Liu, S., Xie, Z., Chen, J., et al. (2018). FERONIA Receptor
- Kinase Contributes to Plant Immunity by Suppressing Jasmonic Acid Signaling in
- 420 Arabidopsis thaliana. *Curr. Biol.* 28, 3316-3324.e6. doi: 10.1016/j.cub.2018.07.078.
- Haruta, M., Sabat, G., Stecker, K., Minkoff, B. B., and Sussman, M. R. (2014). A Peptide
- Hormone and Its Receptor Protein Kinase Regulate Plant Cell Expansion. *Science* 343, 408-
- 423 411. doi: 10.1126/science.1244454.
- Henriques, R., Magyar, Z., Monardes, A., Khan, S., Zalejski, C., Orellana, J., et al. (2010).
- 425 Arabidopsis S6 kinase mutants display chromosome instability and altered RBR1-E2F
- 426 pathway activity. *EMBO J.* 29, 2979–2993. doi: 10.1038/emboj.2010.164.

- Homma, K., Suzuki, K., and Sugawara, H. (2011). The autophagy database: An all-inclusive
- 428 information resource on autophagy that provides nourishment for research. *Nucleic Acids*
- 429 Res. 39. doi: 10.1093/nar/gkq995.
- 430 Keinath, N. F., Kierszniowska, S., Lorek, J., Bourdais, G., Kessler, S. A., Shimosato-Asano, H.,
- et al. (2010). PAMP (Pathogen-associated Molecular Pattern)-induced changes in plasma
- membrane compartmentalization reveal novel components of plant immunity. J. Biol.
- 433 *Chem.* 285, 39140–39149. doi: 10.1074/jbc.M110.160531.
- Kessler, S. A., Shimosato-Asano, H., Keinath, N. F., Wuest, S. E., Ingram, G., Panstruga, R. et
- al. (2010). Conserved Molecular Components for Pollen Tube Reception and Fungal
- 436 Invasion. *Science* 330, 968-971. doi: 10.1126/science.1195211.
- 437 Li, C., Wu, H. M., and Cheung, A. Y. (2016). FERONIA and her pals: Functions and
- 438 mechanisms. *Plant Physiol.* 171, 2379–2392. doi: 10.1104/pp.16.00667.
- Li, F., Chung, T., and Vierstra, R.D. (2014). AUTOPHAGY-RELATED 11 plays a critical role
- in general autophagy- and senescence-induced mitophagy in Arabidopsis. *Plant Cell* 26,
- 441 788-807. doi: 10.1105/tpc.113.120014.
- Li, X., Cai, W., Liu, Y., Li, H., Fu, L., Liu, Z., et al. (2017). Differential TOR activation and cell
- proliferation in Arabidopsis root and shoot apexes. *Proc. Natl. Acad. Sci. USA* 114, 2765–
- 444 2770. doi: 10.1073/pnas.1618782114.
- Liao, C., Wang, P., Yin, Y., and Bassham, D. C. (2022). Interactions between autophagy and
- phytohormone signaling pathways in plants. FEBS Lett. doi: 10.1002/1873-3468.14355.
- Lin, W., Tang, W., Pan, X., Huang, A., Gao, X., Anderson, C. T., et al. (2022). Arabidopsis
- pavement cell morphogenesis requires FERONIA binding to pectin for activation of ROP
- GTPase signaling. Curr. Biol. 32, 497-507.e4. doi: 10.1016/j.cub.2021.11.030.
- Lin, Y., Guo, R., Ji, C., Zhou, J., and Jiang, L. (2021). New insights into AtNBR1 as a selective
- autophagy cargo receptor in Arabidopsis. *Plant Signal. Behav.* 16, e1839226. doi:
- 452 10.1080/15592324.2020.1839226.
- Lindner, H., Müller, L. M., Boisson-Dernier, A., and Grossniklaus, U. (2012). CrRLK1L
- receptor-like kinases: Not just another brick in the wall. Curr. Opin. Plant Biol. 15, 659–
- 455 669. doi: 10.1016/j.pbi.2012.07.003.
- Liu, Y., and Bassham, D. C. (2010). TOR is a negative regulator of autophagy in Arabidopsis
- 457 thaliana. *PLoS ONE* 5, e11883. doi: 10.1371/journal.pone.0011883.

- Liu, Y., and Bassham, D. C. (2012). Autophagy: Pathways for self-eating in plant cells. *Annu*.
- 459 *Rev. Plant Biol.* 63, 215–237. doi: 10.1146/annurev-arplant-042811-105441.
- Liu, Y., Burgos, J. S., Deng, Y., Srivastava, R., Howell, S. H., and Bassham, D. C. (2012).
- Degradation of the endoplasmic reticulum by autophagy during endoplasmic reticulum
- stress in Arabidopsis. *Plant Cell* 24, 4635–4651. doi: 10.1105/tpc.112.101535.
- Luo, S., Li, X., Zhang, Y., Fu, Y., Fan, B., Zhu, C., et al. (2021). Cargo recognition and function
- of selective autophagy receptors in plants. *Int. J. Mol. Sci.* 22, 1–17. doi:
- 465 10.3390/ijms22031013.
- 466 Mahfouz, M. M., Kim, S., Delauney, A. J., and Verma, D. P. S. (2006). Arabidopsis TARGET of
- RAPAMYCIN interacts with RAPTOR, which regulates the activity of S6 kinase in
- response to osmotic stress signals. *Plant Cell* 18, 477–490. doi: 10.1105/tpc.105.035931.
- Marshall, R. S., and Vierstra, R. D. (2018). Annual Review of Plant Biology Autophagy: The
- 470 Master of Bulk and Selective Recycling. *Annu. Rev. Plant Biol* 69, 173–208. doi:
- 471 10.1146/annurev-arplant-042817.
- 472 Martínez Pacheco, J., Song, L., Berdion Gabarain, V., Manuel Peralta, J., Urzúa Lehuedé, T.,
- Angel Ibeas, M., et al. (2022). Cell surface receptor kinase FERONIA linked to nutrient
- sensor TORC1 signaling controls root hair growth at low temperature in Arabidopsis
- 475 thaliana. *bioRxiv*. doi: 10.1101/2022.01.10.475584.
- 476 Masachis, S., Segorbe, D., Turrà, D., Leon-Ruiz, M., Fürst, U., el Ghalid, M., et al. (2016). A
- fungal pathogen secretes plant alkalinizing peptides to increase infection. *Nat. Microbiol.* 1,
- 478 16043. doi: 10.1038/nmicrobiol.2016.43.
- Nolan, T. M., Brennan, B., Yang, M., Chen, J., Zhang, M., Li, Z., et al. (2017). Selective
- Autophagy of BES1 Mediated by DSK2 Balances Plant Growth and Survival. Dev. Cell 41,
- 481 33–46. doi: 10.1016/j.devcel.2017.03.013.
- Pu, Y., Luo, X., and Bassham, D. C. (2017). TOR-dependent and -independent pathways
- 483 regulate autophagy in Arabidopsis thaliana. Front. Plant Sci. 8, 1204. doi:
- 484 10.3389/fpls.2017.01204.
- 485 Ren, M., Qiu, S., Venglat, P., Xiang, D., Feng, L., Selvaraj, G., et al. (2011). Target of
- rapamycin regulates development and ribosomal RNA expression through kinase domain in
- 487 Arabidopsis. *Plant Physiol.* 155, 1367–1382. doi: 10.1104/pp.110.169045.

- 488 Schepetilnikov, M., Makarian, J., Srour, O., Geldreich, A., Yang, Z., Chicher, J., et al. (2017).
- GTPase ROP 2 binds and promotes activation of target of rapamycin, TOR, in response to
- 490 auxin. *EMBO J.* 36, 886–903. doi: 10.15252/embj.201694816.
- 491 Shi, L., Wu, Y., and Sheen, J. (2018). TOR signaling in plants: conservation and innovation.
- 492 *Dev.* 145, dev160887. doi: 10.1242/dev.160887.
- Shih, H. W., Miller, N. D., Dai, C., Spalding, E. P., and Monshausen, G. B. (2014). The receptor-
- like kinase FERONIA is required for mechanical signal transduction in Arabidopsis
- 495 seedlings. Curr. Biol. 24, 1887–1892. doi: 10.1016/j.cub.2014.06.064.
- 496 Shin, S. Y., Park, J. S., Park, H. bin, Moon, K. B., Kim, H. S., Jeon, J. H., et al. (2021).
- FERONIA Confers Resistance to Photooxidative Stress in Arabidopsis. *Front. Plant Sci.*
- 498 12, 714938. doi: 10.3389/fpls.2021.714938.
- 499 Solis-Miranda, J., and Quinto, C. (2021). The CrRLK1L subfamily: One of the keys to versatility
- in plants. *Plant Physiol. Biochem.* 166, 88–102. doi: 10.1016/j.plaphy.2021.05.028.
- 501 Son, O., Kim, S., Kim, D., Hur, Y. S., Kim, J., and Cheon, C. I. (2018). Involvement of TOR
- signaling motif in the regulation of plant autophagy. *Biochem. Biophys. Res. Commun.* 501,
- 503 643–647. doi: 10.1016/j.bbrc.2018.05.027.
- 504 Song, L., Xu, G., Li, T., Zhou, H., Lin, Q., Chen, J., et al. (2022). The RALF1-FERONIA
- 505 Complex Interacts with and Activates TOR Signaling in Response to Low Nutrients. *Mol.*
- 506 *Plant.* doi: 10.1016/j.molp.2022.05.004.
- Song, Y., Wilson, A. J., Zhang, X. C., Thoms, D., Sohrabi, R., Song, S., et al. (2021). FERONIA
- restricts Pseudomonas in the rhizosphere microbiome via regulation of reactive oxygen
- species. *Nat. Plants* 7, 644–654. doi: 10.1038/s41477-021-00914-0.
- 510 Soto-Burgos, J., and Bassham, D. C. (2017). SnRK1 activates autophagy via the TOR signaling
- pathway in Arabidopsis thaliana. *PLoS ONE* 12, e0182591. doi:
- 512 10.1371/journal.pone.0182591.
- 513 Soto-Burgos, J., Zhuang, X., Jiang, L., and Bassham, D. C. (2018). Dynamics of autophagosome
- formation. *Plant Physiol.* 176, 219–229. doi: 10.1104/pp.17.01236.
- 515 Stegmann, M., Monaghan, J., Smakowska-Luzan, E., Rovenich, H., Lehner, A., Holton, N., et al.
- 516 (2017). The receptor kinase FER is a RALF-regulated scaffold controlling plant immune
- signaling. *Science* 355, 287–289. doi: 10.1126/science.aal2541.

- Tang, W., Lin, W., Zhou, X., Guo, J., Dang, X., Li, B., et al. (2022). Mechano-transduction via
- the pectin-FERONIA complex activates ROP6 GTPase signaling in Arabidopsis pavement
- 520 cell morphogenesis. *Curr. Biol.* 32, 508-517.e3. doi: 10.1016/j.cub.2021.11.031.
- van Leene, J., Han, C., Gadeyne, A., Eeckhout, D., Matthijs, C., Cannoot, B., et al. (2019).
- Capturing the phosphorylation and protein interaction landscape of the plant TOR kinase.
- 523 *Nat. Plants* 5, 316–327. doi: 10.1038/s41477-019-0378-z.
- 524 Wang, P., Clark, N. M., Nolan, T. M., Song, G., Bartz, P. M., Liao, C.-Y., et al. (2022).
- Integrated omics reveal novel functions and underlying mechanisms of the receptor kinase
- FERONIA in *Arabidopsis thaliana*. *Plant Cell*. doi: 10.1093/plcell/koac111.
- Wang, P., Mugume, Y., and Bassham, D. C. (2018). New advances in autophagy in plants:
- Regulation, selectivity and function. Semin. Cell Dev. Biol. 80, 113–122. doi:
- 529 10.1016/j.semcdb.2017.07.018.
- 530 Wang, P., Nolan, T. M., Clark, N. M., Guo, H., Bassham, D. C., Walley, J. W., et al. (2021). The
- F-box E3 ubiquitin ligase BAF1 mediates the degradation of the brassinosteroid-activated
- transcription factor BES1 through selective autophagy in Arabidopsis. *Plant Cell* 33, 3532–
- 533 3554. doi: 10.1093/plcell/koab210.
- Wu, F.H., Shen, S.C., Lee, L.Y., Lee, S.H., Chan, M.T., and Lin, C.S. (2009). Tape-Arabidopsis
- sandwich a simpler Arabidopsis protoplast isolation method. *Plant Methods* 5, 16. doi:
- 536 10.1186/1746-4811-5-16.
- 537 Xia, F., Zeng, B., Liu, H., Qi, H., Xie, L., Yu, L., et al. (2020). SINAT E3 Ubiquitin Ligases
- Mediate FREE1 and VPS23A Degradation to Modulate Abscisic Acid Signaling. *Plant Cell*
- 539 32, 3290–3310. doi: 10.1105/tpc.20.00267.
- Xie, Y., Sun, P., Li, Z., Zhang, F., You, C., and Zhang, Z. (2022). FERONIA Receptor Kinase
- Integrates with Hormone Signaling to Regulate Plant Growth, Development, and Responses
- to Environmental Stimuli. *Int. J. Mol. Sci.* 23, 3730. doi: 10.3390/ijms23073730.
- Xiong, Y., Contento, A. L., Nguyen, P. Q., and Bassham, D. C. (2007). Degradation of oxidized
- proteins by autophagy during oxidative stress in arabidopsis. *Plant Physiol.* 143, 291–299.
- 545 doi: 10.1104/pp.106.092106.
- Yoo, S.D., Cho, Y.H. and Sheen, J. (2007). Arabidopsis mesophyll protoplasts: A versatile cell
- system for transient gene expression analysis. *Nat. Protoc.* 2, 1565-1572. doi:
- 548 10.1038/nprot.2007.199.

- Yu, F., Qian, L., Nibau, C., Duan, Q., Kita, D., Levasseur, K., et al. (2012). FERONIA receptor
- kinase pathway suppresses abscisic acid signaling in Arabidopsis by activating ABI2
- phosphatase. *Proc. Natl. Acad. Sci. USA* 109, 14693–14698. doi:
- 552 10.1073/pnas.1212547109.
- 553 Zhang, X., Peng, H., Zhu, S., Xing, J., Li, X., Zhu, Z., et al. (2020). Nematode-Encoded RALF
- Peptide Mimics Facilitate Parasitism of Plants through the FERONIA Receptor Kinase.
- 555 *Mol. Plant* 13, 1434–1454. doi: 10.1016/j.molp.2020.08.014.
- Zhao, C., Zayed, O., Yu, Z., Jiang, W., Zhu, P., Hsu, C. C., et al. (2018). Leucine-rich repeat
- extensin proteins regulate plant salt tolerance in Arabidopsis. *Proc. Natl. Acad. Sci. USA*
- 558 115, 13123–13128. doi: 10.1073/pnas.1816991115.
- 559 Zhou, J., Zhang, Y., Qi, J., Chi, Y., Fan, B., Yu, J. Q., et al. (2014). E3 Ubiquitin Ligase CHIP
- and NBR1-Mediated Selective Autophagy Protect Additively against Proteotoxicity in Plant
- Stress Responses. *PLoS Genet.* 10, e1004478. doi: 10.1371/journal.pgen.1004116.
- Zhuang, X., Chung, K. P., Luo, M., and Jiang, L. (2018). Autophagosome Biogenesis and the
- Endoplasmic Reticulum: A Plant Perspective. *Trends Plant Sci.* 23, 677–692. doi:
- 564 10.1016/j.tplants.2018.05.002.

566 FIGURE LEGENDS

565

- Figure 1. Comparison of autophagy-related genes with transcriptome and proteome of fer-4. A,
- Venn diagram showing the overlaps among autophagy-related genes (Homma et al., 2011) and
- differentially expressed transcripts and proteins in *fer-4* mutant. B, Selected genes involved in
- autophagy and their changes in two sets of differentially expressed data (UP: increased levels in
- 571 *fer-4* mutant; DN: decreased levels in *fer-4* mutant).
- Figure 2. FER negatively regulates autophagy under sucrose starvation. A, Representative
- 574 confocal microscopic images of WT and *fer-4* with autophagosome marker GFP-ATG8e, under
- 575 control (SUC+) and sucrose starvation (SUC-) conditions. The Lavender arrows indicate
- autophagosomes. Scale = $40 \mu m$. B, Quantification of autophagosomes of the 10-day-old
- seedlings from A. Data are shown as means \pm SEM from 3 biological replicates, with 6-12
- 578 images per replicate. Different letters indicate significant difference among groups subjected to
- one-way ANOVA Tukey's multiple range tests (p < 0.05). C, Western blot showing the

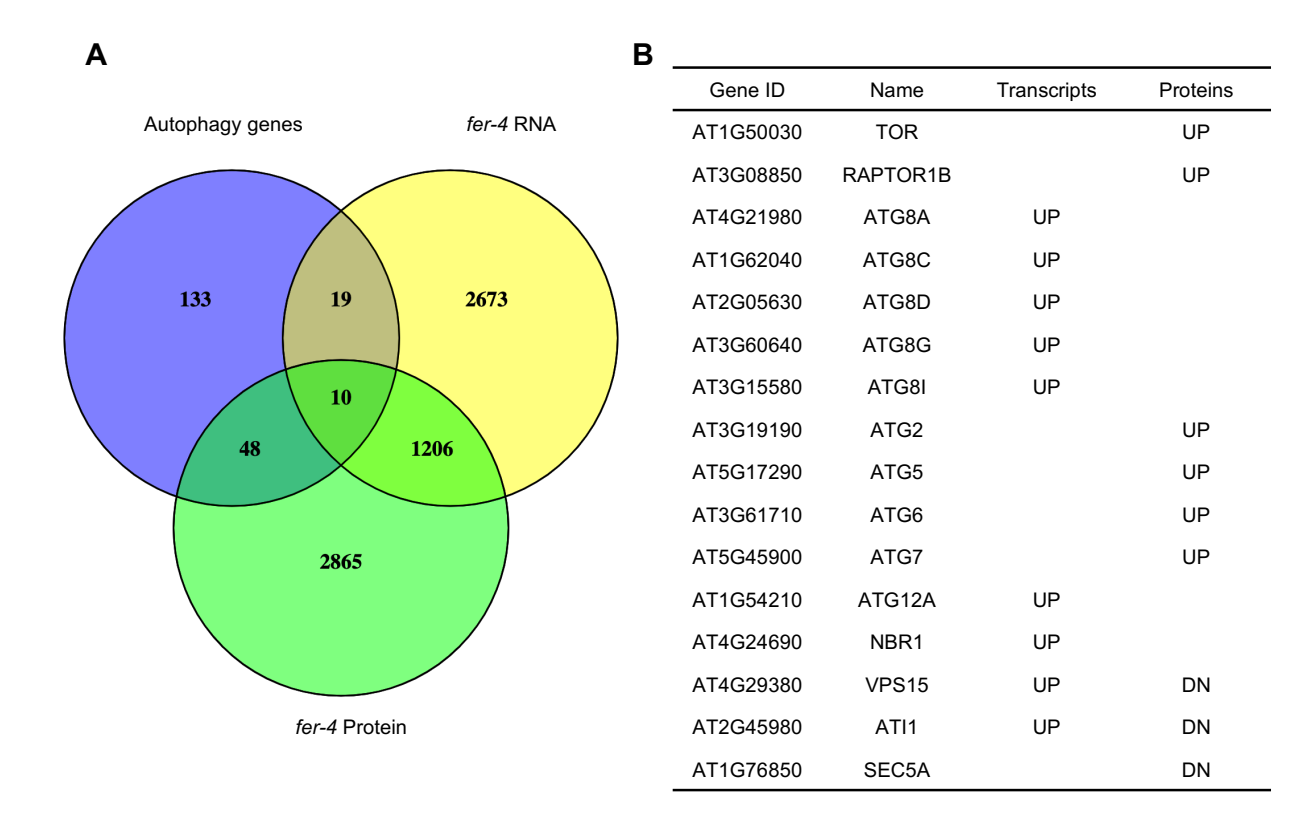
580 decreased FER protein levels in multiple T2 lines of FER-miRNA/GFP-ATG8e using anti-FER 581 antibody (Guo et al., 2018). Lines #1, #2 and #4 were used for further autophagy analysis. 582 Rubisco was used as loading control. D, Quantification of autophagosomes of the 10-day-old 583 seedlings from C with or without sucrose and grown in dark for 3 days. Data are shown as means 584 ± SEM from 5-12 seedlings, with 2-3 images per seedlings. Different letters indicate significant 585 difference among groups subjected to one-way ANOVA Tukey's multiple range tests (p < 0.05). 586 E. GFP-ATG8e cleavage assays showing the increased autophagic flux in fer-4 mutant. Seven-587 day-old WT GFP-ATG8e and fer-4 GFP-ATG8e seedlings were subjected to ½ LS liquid 588 medium without sucrose for 6, 12, and 24 hours in dark. The total proteins were extracted and 589 separated by SDS-PAGE gels followed by immunoblotting with anti-GFP antibody. Ponceau S 590 staining serves as protein loading control. The values below the blots are the ratios of free GFP 591 over GFP-ATG8e. This experiment was carried out two times with similar results. 592 593 Figure 3. FER negatively regulates autophagy under AZD8055 treatment. A, Quantification of 594 autophagosomes. Seven-day-old seedlings of WT GFP-ATG8e and fer-4 GFP-ATG8e grown on 595 $\frac{1}{2}$ LS plates were transferred to control liquid $\frac{1}{2}$ LS or $\frac{1}{2}$ LS with 1 μ M AZD8055 for 6 hours. 596 Data are shown as means \pm SEM from 11-13 seedlings, with 2-3 images per seedlings. Different 597 letters indicate significant difference among groups subjected to one-way ANOVA Tukey's 598 multiple range tests (p < 0.05). B, GFP-ATG8e cleavage assays of seedlings from A. The total 599 proteins were extracted and separated by SDS-PAGE gels followed by immunoblotting with 600 anti-GFP antibody. Ponceau S staining serves as protein loading control. The values below the 601 blots are the ratios of free GFP over GFP-ATG8e. This experiment was carried out two times 602 with similar results. 603 604 Figure 4. FER and TOR cooperate in plant growth and autophagy. A, Hypergeometric tests on 605 the comparisons of AZD-regulated transcripts and differentially expressed transcripts or proteins 606 in fer-4 mutant. Significant overlaps are highlighted in yellow. DE: differentially expressed; NS: 607 not significant. B, Venn diagram showing the comparison of differentially expressed transcripts 608 in fer-4 and differentially expressed genes in response to TOR kinase inhibitor AZD8055 609 treatment (Dong et al., 2015). The red *** represents the overlaps statistically significant with p 610 < 0.001. C, Growth phenotype of 3-week-old plants of WT, fer-4, TOROE and fer-4 TOROE

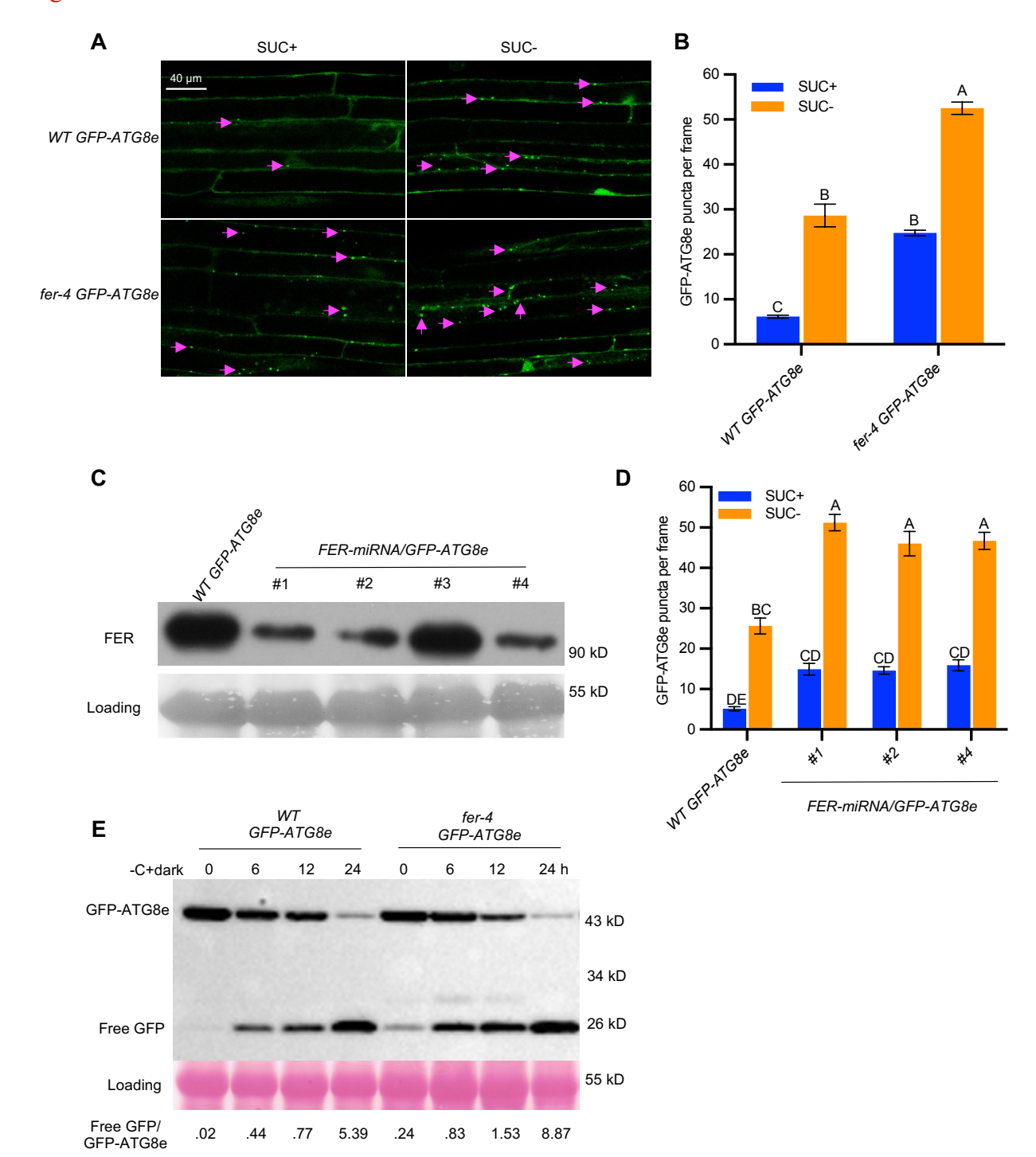
611 double mutant. D, Representative confocal microscopic images of WT, fer-4, TOROE and fer-4 612 TOROE with autophagosome marker GFP-ATG8e, under control (SUC+) and sucrose starvation 613 (SUC-) conditions. The Lavender arrows indicate the autophagosomes. Scale = $40 \mu m$. E, 614 Quantification of autophagosomes in different genotypes expressing GFP-ATG8e from 10-day-615 old seedlings with or without sucrose for 3 days. Data are shown as means \pm SEM from 3 616 biological replicates, with 14-31 images per replicate. Different letters indicate significant 617 difference among groups subjected to one-way ANOVA Tukey's multiple range tests (p < 0.05). 618 619 Figure 5. FER-GFP inhibits sucrose starvation-induced autophagy but not the constitutive 620 autophagy in raptor 1b. A-B, Quantification of protoplasts with ATG8e labeled autophagy. A, 621 GFP control or FER-GFP was co-expressed with mCherry-ATG8e in Col-0 protoplasts, treated 622 without or with 0.5% (w/v) sucrose for 36 hours before microscopy. B, GFP control or FER-623 GFP was co-expressed with mCherry-ATG8e in Col-0 and raptor1b protoplasts, followed by 20 624 hours incubation before microscopy. Protoplasts with more than three visible autophagosomes 625 were counted as being active for autophagy. A total of 100 well-expressed protoplasts were 626 observed for each treatment per genotype, and the percentage of protoplasts with active 627 autophagy was calculated. Data are shown as means \pm SEM from 3-4 biological replicates. 628 Different letters indicate significant difference among groups subjected to one-way ANOVA 629 Tukey's multiple range tests (p < 0.05). 630 631 Figure 6. fer-4 was more sensitive to AZD in root growth assay. A, Images of 7-day-old seedlings of WT, fer-4, TOROE and fer-4 TOROE grown on control ½ MS plates or plates 632 633 containing 1 µM AZD8055. B, Root length measured from seedlings of A using ImageJ. Data 634 are shown as means \pm SEM (n=12). Different letters indicate significant difference among 635 groups subjected to one-way ANOVA Tukey's multiple range tests (p < 0.05). C, Root growth 636 inhibition by AZD8055 was analyzed using a generalized linear model (glm package in R) with 637 genotype and treatment (Control or AZD) as fixed factors. The genotypes were categorized as 638 significantly differentially responsive to AZD if they had a genotype-by-treatment interaction p-639 value < 0.05 compared to all other genotypes (n=12).

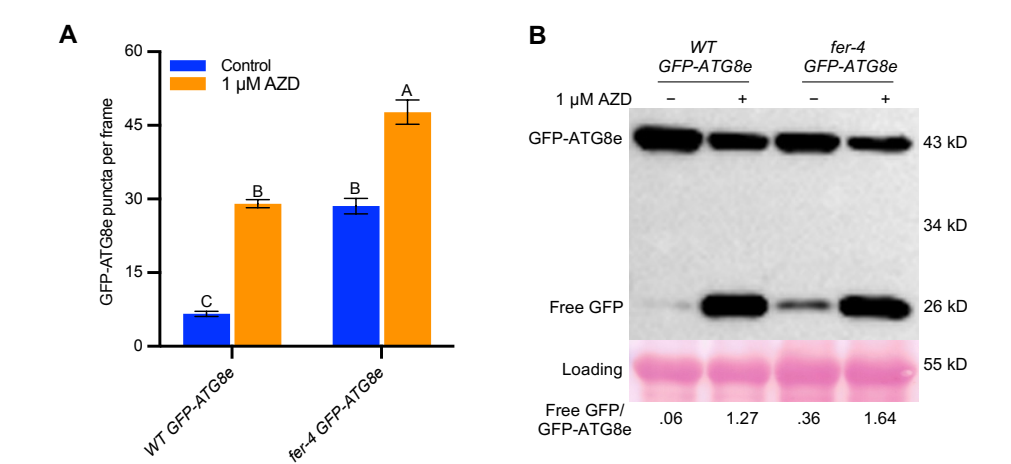
641 Figure 7. S6K1/2 phosphorylation by TOR was decreased in fer-4 mutant. A, Western blot 642 showing testing of anti-S6K1/2 and anti-P-S6K1/2 (phosphorylated S6K1/2) antibodies in WT 643 with or without 5 µM AZD8055 for 3 h. Ponceau S staining was used as loading control. B-C, 644 Western blot showing phosphorylated and non-phosphorylated S6K1 in 10-day-old seedlings of indicated genotypes, with and without different concentrations of AZD8055 treatment for 1 h (B) 645 646 or under control or sucrose-starvation conditions (C). The ratios of P-S6K1/S6K1 were obtained 647 using ImageJ, and the ratio in WT was set as 1.0 in (B) and 1.0 for TOROE in (C). IWS1 protein 648 was used as loading control with anti-IWS1 (Wang et al., 2021). D, A working model showing a 649 possible mechanism in which FER activates TOR/RAPTOR1B to inhibit autophagy. 650 651 Supplemental Figure 1. Comparison of AZD8055 regulated genes with another two sets of 652 published transcriptomes of fer-4. A, Venn diagram comparison of differentially expressed 653 transcripts in 10-day-old fer-4 seedlings (Wang et al., 2022) with differentially expressed genes 654 in response to TOR kinase inhibitor AZD8055 treatment (Dong et al., 2015). B-C, Venn diagram 655 comparisons of the co-regulated genes from A and from Figure 4B. D, Venn diagram 656 comparison of differentially expressed transcripts in fer-4 published by Guo et al. (2018) with 657 differentially expressed genes in response to TOR kinase inhibitor AZD8055 treatment (Dong et 658 al., 2015). E-F, Venn diagram comparisons of the co-regulated genes from D and from Figure 659 4B. 660 661 Supplemental Figure 2. S6K1 phosphorylation in WT and TOR OE seedlings. Seven-day-old 662 seedlings were treated with 0.2 µM AZD8055 for 2 hours. Ponceau S staining was used as 663 loading control. The ratios of P-S6K1/S6K1 were obtained using ImageJ, and the ratio in WT 664 was set as 1.0. 665 666 Supplemental Table 1. List of autophagy-related genes for comparisons with transcriptome and 667 proteome of *fer-4*. 668 669 Supplemental Table 2. List of AZD8055 down-regulated genes for comparisons with 670 transcriptome and proteome of fer-4.

- 672 Supplemental Table 3. List of AZD8055 up-regulated genes for comparisons with transcriptome
- and proteome of *fer-4*.
- 674

Figure 1

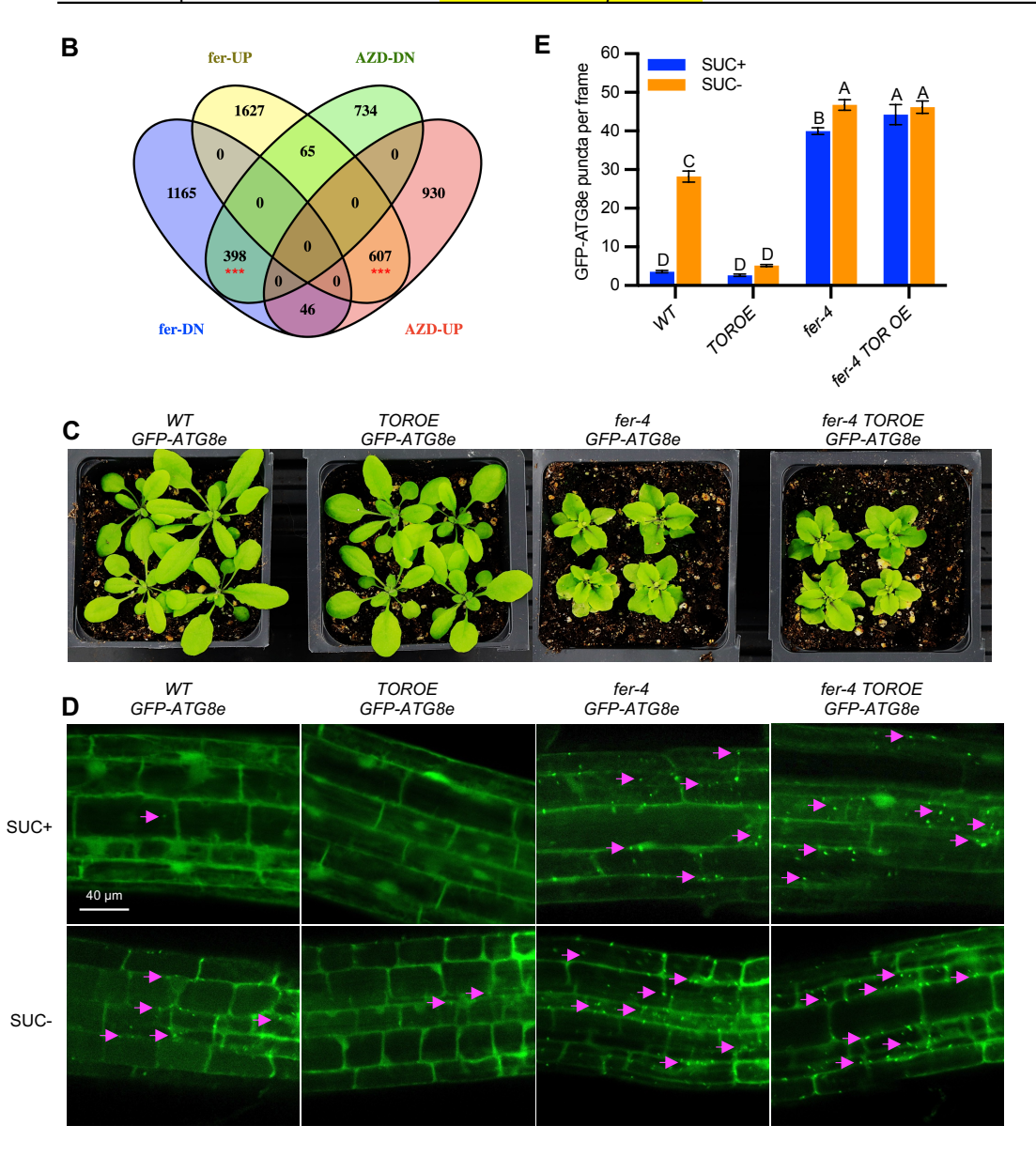


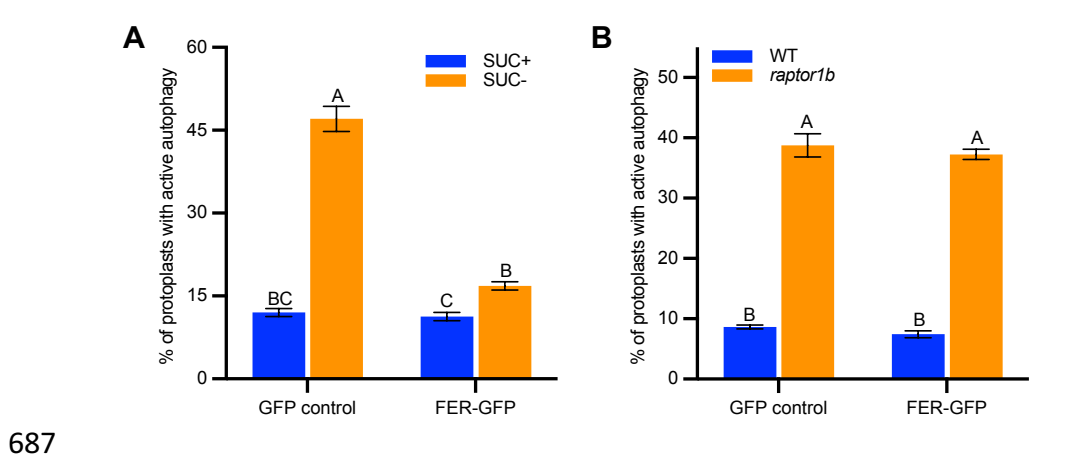




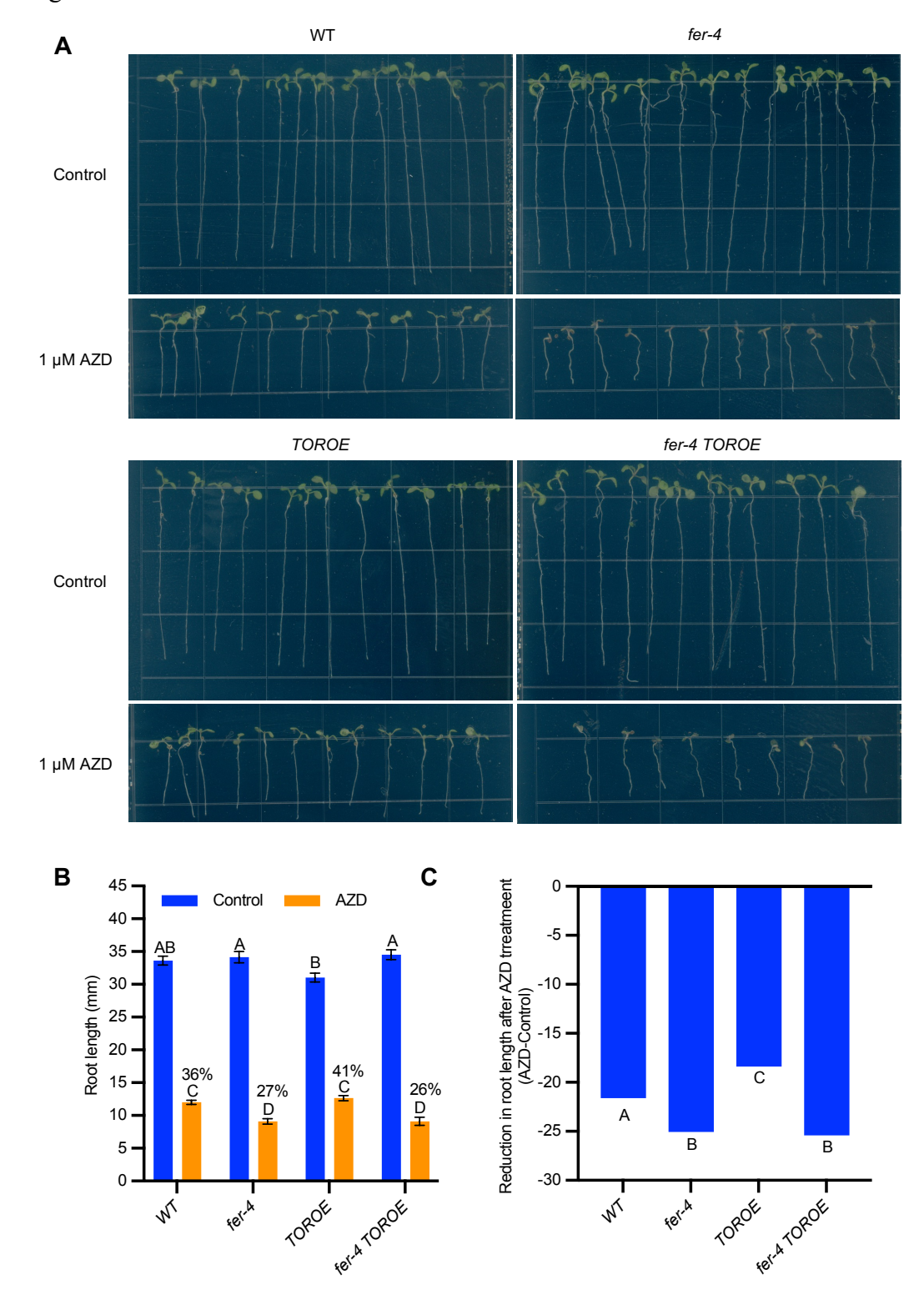
Α

Omics datasets	DE in fer-4	AZD DN in fer-4	Percent AZD DN	p-value	AZD UP in fer-4	Percent AZD UP	<i>p</i> -value
Total DE transcript	3908	463	40%	<i>p</i> <0.001	653	42%	<i>p</i> <0.001
Up in fer-4 transcript	2299	65	14%	NS	607	93%	<i>p</i> <0.001
Dn in fer-4 transcript	1609	398	86%	<i>p</i> <0.001	46	7%	NS
Total DE protein	4133	578	76%	<i>p</i> <0.001	421	82%	<i>p</i> <0.001
Up in fer-4 protein	2349	151	26%	NS	374	89%	<i>p</i> <0.001
Dn in fer-4 protein	1784	427	74%	p<0.001	47	11%	NS





689 Figure 6



P-S6K/S6K

693 694 .63

.42

.15

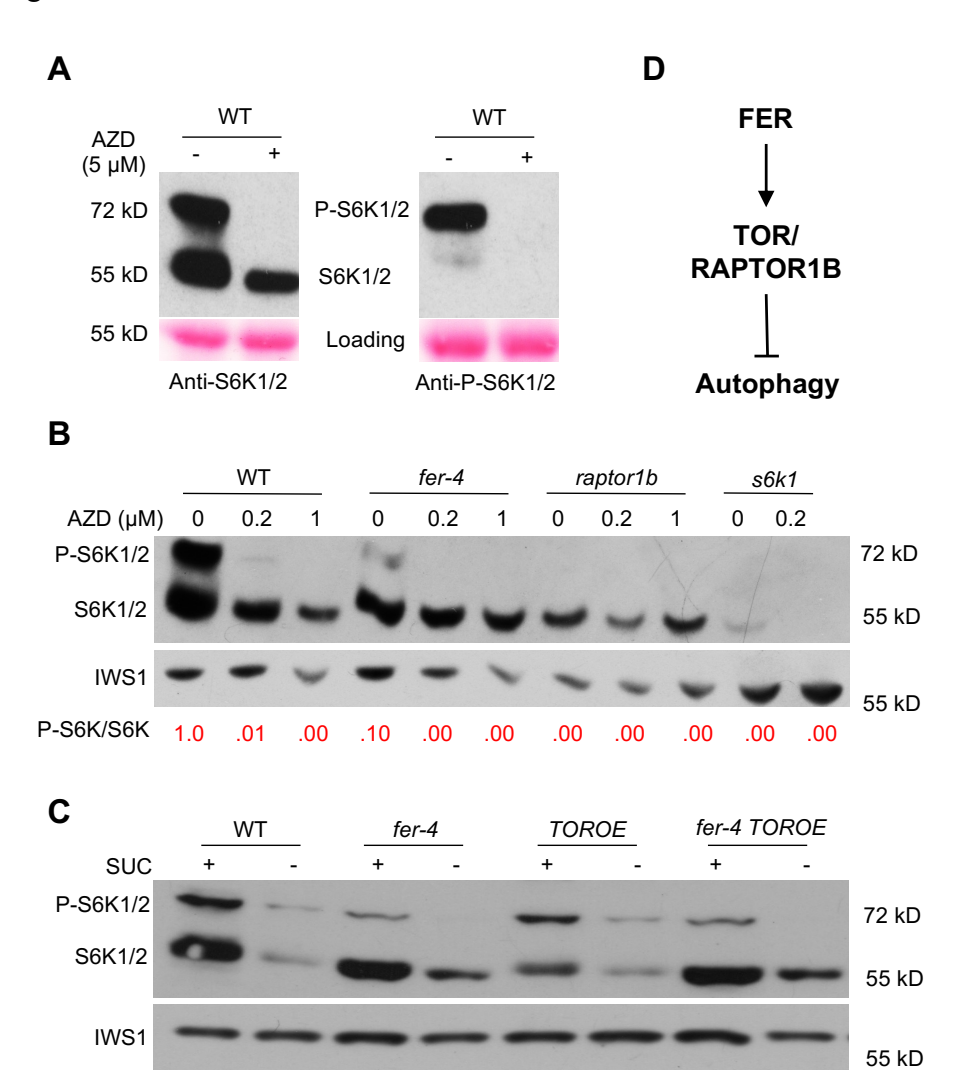
.00

1.0

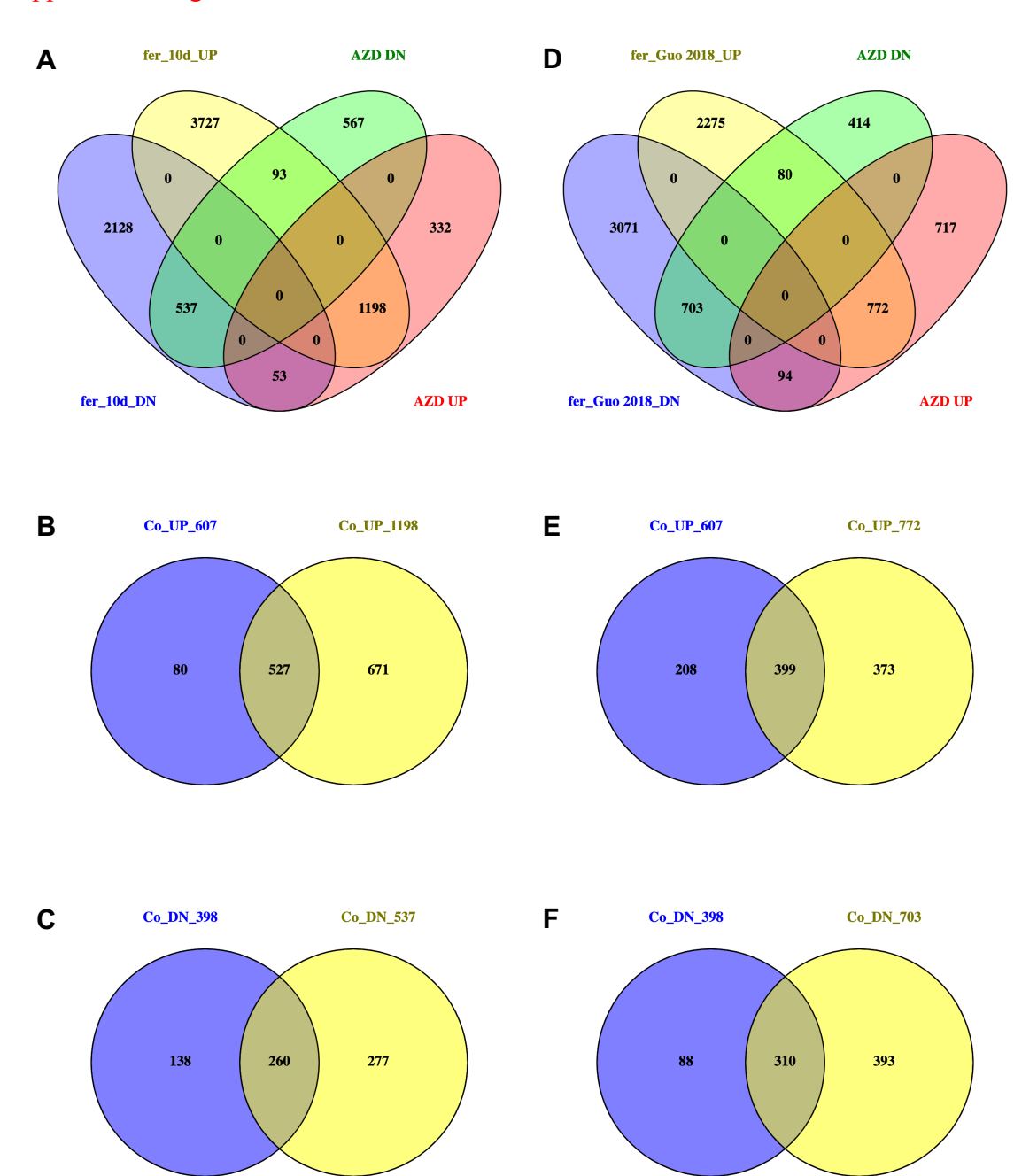
.45

.15

.00



695 Supplemental Figure 1



698 Supplemental Figure 2

